Seafloor characterization and benthic megafaunal distribution of an active submarine canyon and surrounding sectors: The case of Gioia Canyon (Southern Tyrrhenian Sea)

Martina Pierdomenico [a,*], Eleonora Martorelli [b], Carlos Dominguez-Carrió [c], Josep Maria Gili [c], Francesco Latino Chiocci [a]

[a] Department of Earth Sciences, Sapienza University of Rome, P.le A. Moro 5, 00185 Rome, Italy
[b] CNR-IGAG (Istituto di Geologia Ambientale e Geoingegneria), UOS Roma, P.le A. Moro, 5, 00185, Rome, Italy
[c] Institut de Ciències del Mar, Consejo Superior de Investigaciones Cientificas, Pg. Marítim de la Barceloneta 37–49, 08003 Barcelona, Spain
http://dx.doi.org/10.1016/j.jmarsys.2016.01.005

Abstract

In this paper, we used multibeam bathymetry and backscatter, high-resolution seismic profiles, ROV video im- ages and sediment samples to identify the principal morpho-sedimentary features and related megabenthic communities along the upper reach of the Gioia Canyon (depth b 600 m) and the surrounding shelf and slope areas. Interpretation of the multidisciplinary dataset was undertaken to evaluate the relationships between sea- floor characteristics and faunal distribution along a submarine canyon in an active tectonic setting. The results from this study indicate that physical disturbance on the seafloor at the canyon head and surrounding shelf, re- lated to high sedimentation rates and occasional turbidite flows, may limit the variability of megabenthic com- munities. Evidence of diffuse trawl marks over soft sedimentary bottoms indicates anthropogenic impact due to fishing activities, which could explain low abundances of megabenthic species observed locally. The canyon margins and flanks along the continental slope host octocorals Funiculina quadrangularis and Isidella elongata, species that are indicative of vulnerable marine ecosystems (VMEs) and relevant in terms of sustainable manage- ment priorities. At the Palmi Ridge, the occurrence of outcropping rocks and bottom currents related to the pres- ence of Levantine Intermediate Waters, provide conditions for the development of hard-bottom assemblages, including the black coral Antipathella subpinnata and deep-sea sponges fields.

1. Introduction

Submarine canyons are complex and common features along continental margins (Harris and Whiteway, 2011) that act as major conduits for transport of sediment, water masses and organic matter to bathyal and abyssal depths (Shepard and Dill, 1966; Canals et al., 2006).

The complex topography, the complicated hydrodynamic patterns and the enhanced transport processes of submarine canyons contribute to increase habitat heterogeneity, creating a variety of benthic habitats which support high values of benthic faunal biomass and diversity (Rowe et al., 1982; Vetter et al., 2010). Canyon heads and walls can have exposed rocks suitable for fragile sessile filter feeders such as cold water corals and sponges (Gori et al., 2013; Bo et al., 2012b; Huvenne et al., 2011), while soft sediment areas typically host fauna dominated by deposit feeders, scavengers and predators, which benefit from an enhanced food supply (Vetter and Dayton, 1998; Okey, 2003). The upwelling and mixing of water masses due to flow interaction with canyon topography can drive nutrient delivery from deep areas into the euphotic zone, resulting in an enrichment of the water column and pelagic systems (Allen and Durrieu de Madron, 2009). Enhanced local fishery production around canyons when compared to open-slope environments has also been reported (Cartes et al., 2004).

Due to their ecological relevance, submarine canyons are included among topographical features that may support vulnerable marine ecosystems (VMEs) and thus merit special attention in terms of sustainable management (FAO, 2009). Although submarine canyons are recognized for their importance as biological hotspots and their key role in connecting the continental shelf to the deep sea, our understanding of their formation, processes and ecosystems is still relatively limited (De Leo et al., 2010; Harris and Whiteway, 2011; Puig et al., 2014). Due to the difficulty of surveying such complex environments, detailed multidisciplinary studies have only arisen in the last two decades, in parallel with advances in marine technology such as swath bathymetry, remote sensing, long-term moorings and remotely operated vehicles (Ramirez-Llodra et al., 2010).

Faunal distribution and biodiversity within submarine canyons are regulated by a complex interplay of multiple factors, including habitat heterogeneity, seafloor disturbance and food supply (Okey,

2003; McClain and Barry, 2010; De Leo et al., 2014), which in turn depends on a large number of physical factors such as shelf morphology, proximity to river systems, substrate lithology, prevailing oceanographic conditions, sediment transport processes, sedimentation rates, nutrient input and depth (Harris and Whiteway, 2011; Puig et al., 2014). In this sense, different kinds of canyon or diverse sections of a single canyon may vary significantly in their topography, hydrodynamic and sedimentary regimes (Allen et al., 2001; McClain and Barry, 2010; Van Oevelen et al., 2011). This complexity of physical influences can make understanding the various controlling factors that determine the complexity of their faunal assemblages very challenging.

During the present highstand of the sea level, submarine canyons that deeply indent the continental shelf intercept larger amounts of sediment than those having a reduced shelf penetration or that are slope confined (Puig and Palanques, 1998). However, the relationship between the state of activity of a given canyon and the fauna colonizing it is still unclear, and only a limited number of studies have examined the effect of canyon activity upon community composition (Okey, 1997, 2003; Paull et al., 2010a; McClain and Barry, 2010; Van Oevelen et al., 2011; Duffy et al., 2014).

Shelf indenting submarine canyons receiving sediments from fluvial input and/or from along-shelf transport can be sites of intense organic enrichment that, along with the heterogeneity of substrates, represent favorable conditions for the benthic fauna (Vetter and Dayton, 1998, 1999; De Leo et al., 2010). These canyons can also receive enhanced advection of shelf resuspended sediments and be recurrently affected by storm-induced turbidity currents (Xu et al., 2010). Moreover, when these canyons are connected to river sources, they can be exposed to hyperpycnal flows during pulses of river discharge or can be affected by mass flows derived from failures of recently deposited sediments (Kao and Milliman, 2008; Puig et al., 2014 and references therein). Benthic organisms exposed to such events may be physically damaged or displaced and therefore, communities dominated by slow-growing, fragile megafauna may struggle to survive.

In recent years, progress has been made in understanding the geological evolution and the dynamics of present-day physical processes along the Gioia Canyon (Southern Tyrrhenian Sea, Fig. 1) (Colantoni et al., 1992; Gamberi and Marani, 2006, 2008; Morelli et al., 2013; Casalbore et al., 2014; Zaniboni et al., 2014). These studies showed that the Gioia Canyon, indenting the continental shelf up to a very shallow depth of about 10 m, is an active submarine canyon, presently dominated by sediment bypass. In contrast, the knowledge of ecological processes of this region is still lacking. Few ecological investigations were conducted in the Gulf of Gioia (Innamorati et al., 1996; Porporato et al., 2008) and none have been conducted in the Gioia Canyon in particular prior to this work.

For the present study, we used a wide range of data including multibeam bathymetry and backscatter, high-resolution seismic profiles, ROV video images and sediment samples to identify and map the main morphological and depositional features and the associated megabenthic communities along the upper reach of the Gioia Canyon (depth b 600 m) and the surrounding shelf and slope areas.

The aims of this paper are therefore: 1) to present evidence for the ongoing sedimentary and oceanographic processes that control the distribution of the observed seafloor features (e.g. along and across-shore sediment transport processes, action of bottom currents) and 2) to explore the relationships between seafloor conditions and megabenthic communities, in order to evaluate the influence of cross-shelf sediment transport and canyon activity on the benthic fauna in an active tectonic setting characterized by high sedimentation rates.

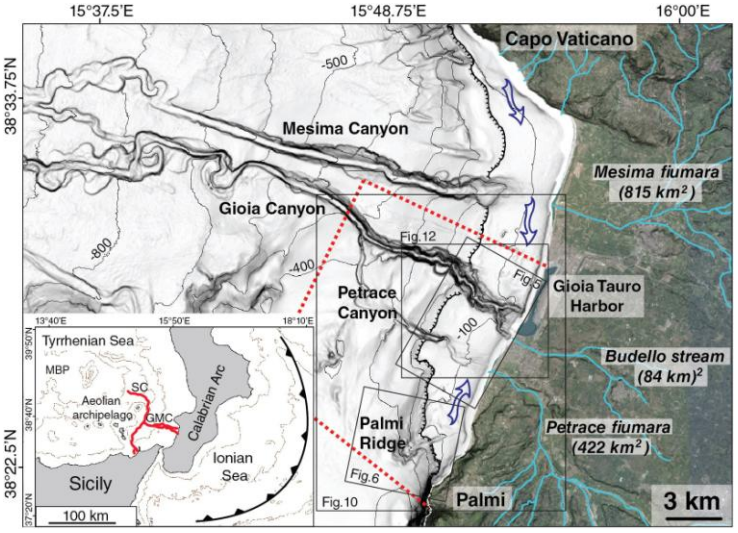

Fig. 1. Bathymetric map of the Gulf of Gioia (Tyrrhenian Calabrian margin) showing the Gioia–Mesima Canyon System and the study area (denoted by the red box). Contour lines every 100 m. The ragged black line indicates the shelf break and blue arrows indicate coastal currents direction (from Lupia Palmieri et al., 1997). Fiumare courses and their catchment basin's areas are also shown. Inset on the bottom right: southern Calabrian margin. The Gioia–Mesima–Stromboli Canyon System is represented by the red line. The bold striped line indicates the subduction of the Ionian crust underneath the Calabrian Arc (modified from Fabbri et al., 1980). Contour lines every 1000 m. GMC – Gioia–Mesima Canyon; SC – Stromboli Canyon; MBP – Marsili Bathyal Plain.

2. Study area

2.1. Geological setting

The Gioia Canyon is part of the Gioia–Mesima–Stromboli canyon system, which extends across the southeastern Tyrrhenian margin for about 120 km from the coastal sector down to the Gioia intraslope basin and the Marsili Bathyal Plain (Fig. 1).

Since the Upper Miocene this area has been affected by complex tectonics related to the opening of the Tyrrhenian Sea back-arc basin, created by the subduction of oceanic crust of the Ionian Sea underneath the Calabrian Arc (Fig. 1) (Fabbri et al., 1980; Doglioni et al., 2004). A regional tectonic uplift that started 0.6 Ma and has been responsible for the high seismicity of the area (Tortorici et al., 1995). The subsidence of the Gioia basin and the uplift in the mainland shaped the continental margin, producing coastal mountain chains, narrow coastal plains and a very narrow to nearly absent continental shelf (Fabbri et al., 1980; Gamberi and Marani, 2006). Sedimentation on the continental margin is characterized by the interplay between sea-level changes, high sedimentation rate and diffuse instability processes due to the Calabrian Arc uplift (Gamberi and Marani, 2006; Casalbore et al., 2014).

The study area (Fig. 1) is located offshore the central sector of the Gulf of Gioia, in the southernmost part of the Calabrian Arc. The Gulf of Gioia is bounded by Capo Vaticano and Palmi promontories (Fig. 1), where pre-Mesozoic metamorphic and plutonic rocks outcrop shaping the coast into high cliffs and pocket beaches (D'Alessandro et al., 2002). Conversely, along the coastal plain, the bedrock is deeply buried under the marine sediments of Late Pliocene to Mid-Pleistocene age and by alluvial Quaternary deposits of the Gioia Tauro half-graben (Colantoni et al., 1992); here wide gravelly beaches are present (D'Alessandro et al., 2002). The region is drained by gravel-bed streams locally called fiumare, whose catchments develop mainly in high mountain areas, still subject to tectonic uplift and diffuse mass wasting (Tortorici et al., 1995). Their flashy flow regime (Poff et al., 1997) is mainly controlled by episodic catastrophic flash floods (Sabato and Tropeano, 2004). Gamberi and Marani (2008) hypothesized that mass flows fed by the two main fiumara present on the study area (the Mesima and the Petrace fiumara, Fig. 1) were responsible for the evolution and present day activity of the Gioia–Mesima canyon system.

2.2. The Gioia–Mesima canyon system

The Gioia–Mesima canyon system (Fig. 1) incises the shelf and slope of the Gioia Basin and the two courses of the Gioia Canyon and the Mesima Canyon run parallel, changing from straight to meandering geometry at around 700 m depth, until they merge in a single lower reach at 1000 m depth (Fabbri et al., 1980). While the Mesima Canyon is an abandoned valley hanging on the Gioia Canyon (Morelli et al., 2013), the Gioia Canyon is an erosive feature acting chiefly as a sediment bypass conduit (Gamberi and Marani, 2008; Colantoni et al., 1992).

The canyon head is composed of two branches that deeply incise the continental shelf starting from a depth of only 10 m. Both branches are located in front of the Gioia Tauro Harbor, one of the largest shipping terminals of the Mediterranean Sea (Fera and De Paoli, 2012, Fig. 1). The accumulation of sediment at the head of the Gioia Canyon during the harbor construction led to a submarine slide in 1977, with an estimate volume of 5.5×10^6 m^3 of sediment (Colantoni et al., 1992). The event generated a turbidity current that travelled downslope at an estimated speed of 15 to 17 km/h, breaking a submarine cable located on the Gioia Canyon floor at 600 m depth (Colantoni et al., 1992). Apart from major failure events, recent activity of the Gioia Canyon is related to the sediment transported by long-shore currents that can be trapped within the canyon (D'Alessandro et al., 2002). High-energy sedimentary dynamics at the canyon head are suggested by the presence of crescent shaped bedforms within its thalweg (Casalbore et al., 2014).

2.3. Oceanographic setting

The most relevant water masses that flow in the Southern Tyrrhenian Sea are: 1) MAW—Modified Atlantic Water, surface water of Atlantic origin that occupies the upper part of the water column; 2) LIW–Levantine Intermediate Water, intermediate water that originates in the Levantine Basin occupying a depth range of 200–700 m; 3) TDW—Tyrrhenian Deep Water, which originates due to complex mixing processes between the LIW and Western Mediterranean Deep Water (WMDW), filling the basin down to the bottom (Sparnocchia et al., 1999). An outflow of LIW between 130 and 400 m depth, coming from the Ionian side of the Strait of Messina and driven by tidal currents, was described in the study area by Marullo and Santoleri (1986). High velocities associated with the tidal currents and their interaction with the complex bathymetry of the Messina Strait generate nonlinear internal waves that propagate northward parallel to the Calabrian margin (Brandt et al., 1997). The breaking of these internal waves is thought to be responsible for the peculiar thermal front observed by Marullo and Santoleri (1986) south of Capo Vaticano.

3. Data and methods

3.1. Geophysical data

Geophysical data used in this study, including multibeam bathymetry, backscatter data and seismic profiles (Fig. 2), were acquired during several cruises conducted in the area between 2009 and 2012 on board of the R/V Urania (CNR, Italy), in the framework of the Magic project (MArine Geohazard Along the Italian Coasts, Chiocci and Ridente, 2011).

The high-resolution bathymetric data were acquired using multibeam systems operated at different frequencies (from 50 to 455 kHz), with DGPS- or RTK-positioning. Raw multibeam data were processed using Caris HIPS and SIPS® 7.0 software in order to produce a digital elevation model (DEM) of the study area with a 10 m horizontal resolution (Fig. 2A). A 10 m horizontal resolution slope map (Fig. 2B) was extracted from the bathymetric data and used to interpret different geomorphological features.

Backscatter data were collected by a Simrad EM710 Multibeam system (70–100 kHz) and processed using the software Geocoder® (Fonseca and Calder, 2005). Raw backscatter data were corrected to remove variable acquisition gains, power levels, insonification areas and grazing angles. Geometric corrections were applied to compensate for navigation and transducer attitude before the mosaicking of the data. The final product was a backscatter mosaic with a 2 m horizontal resolution (Fig. 3).

High-resolution seismic profiles (Fig. 2) were acquired using a Benthos Chirp III subbottom profiler, equipped with a dual modulated frequency ranging between 2 and 20 kHz and a maximum penetration of about 50 m. The vertical resolution was up to 1–2 m.

3.2. Groundtruth data

Remotely operated vehicle (ROV) images (Fig. 2, Table 1) and sediment samples (Fig. 2, Table 2) were collected in 2013 during the "Tygraf" cruise on board of the R/V Urania (CNR, Italy; http://www.ritmare.it), except for two video transects acquired during a previous cruise in the framework of the Magic Project (Table 1).

3.2.1. ROV video data

ROV data include 14 video transects. The video images used for this study were acquired by means of a standard definition video camera (Sony CCD 1/3") mounted on the ROV POLLUX III, towed behind the survey vessel at an average speed of 0.3 knots. The position of the ROV was estimated from the vessel positioning system with a maximum estimated error of ±20 m.

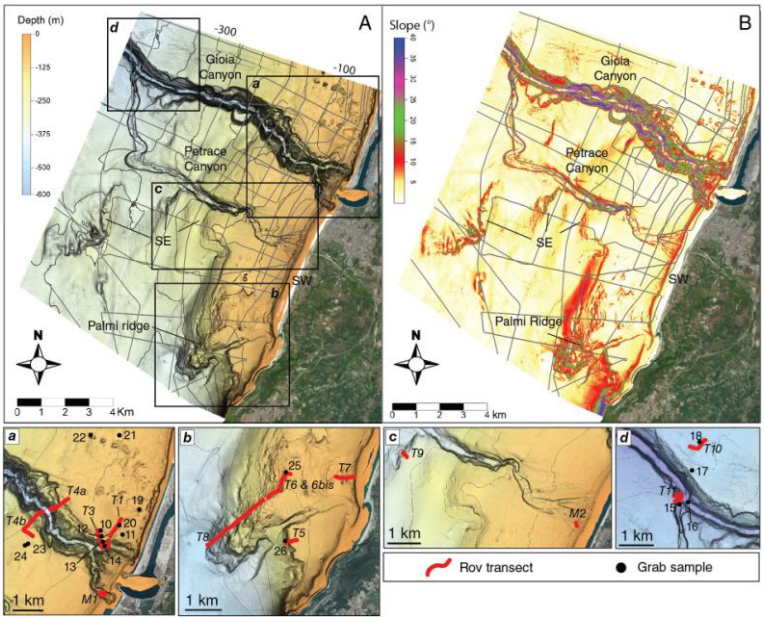

Fig. 2. Bathymetric (A) and slope (B) maps from the study area. The chirp seismic profiles used in this study are shown on the maps (gray lines). The location of ROV transects (red lines) and grab samples (black dots) used in this study is shown in the insets. Contour lines every 50 m. SW −Sedimentary wedge; SE −Slope escarpment.

The video sequences were edited using the software Final Cut Pro (Apple Inc.), removing fragments and excluding pauses in the movement of the vehicle. This procedure ensured an accurate estimate of the total length of each sequence, for which a constant speed was assumed and calculated. The analyses of the video sequences included the description of the seafloor texture, the identification and enumeration of benthic megafauna and the identification of potential anthropogenic impacts (e.g. presence of litter and trawl marks over the seabed).

Based on the video observations, different classes of seafloor types were defined and mapped along the transects. All megafauna observed in the sequences were enumerated and identified to the lowest possible taxon (which corresponded to species, genus, family or higher taxonomic levels in some cases), with the aid of specialists in different groups: sponges (Dr. Iosune Uriz), cnidarians (Dr. Josep-Maria Gili and Dr. Pablo J. López-González) and polychaetes (Dr. Rafael Sardá). When specific taxa could not be easily assigned, a general assignment to morphospecies or morphotype was applied. Lack of an image scaling device (e.g. parallel laser beams) prevented the calculation of the absolute density of megafauna, allowing only relative abundances of the taxa present in the tracks to be determined. The presence of litter and bottom-trawl marks over the seabed was reported along with the identification of the organisms.

All video sequences were split into 50 m length segments based on the vessel position and the timecode of the edited videos. Benthic taxa and the abiotic variables identified (including seafloor type, depth and slope) were assigned to each of these segments, which were thereafter designated as sampling units. Highly mobile taxa were removed from the dataset prior to statistical analyses. Sequences where silt clouds obscured the image or where oscillations of the vehicle did not ensure a constant altitude above the seabed, were considered of poor quality and removed for subsequent analyses.

3.2.1.1. Statistical analyses on ROV video data. To identify the megabenthic assemblages, a hierarchical cluster analysis with group-averaged linkage was performed using a Bray−Curtis similarity matrix derived from the square root transformation of the data. A similarity profile analysis (SIMPROF) was then applied to the resemblance matrix to identify significantly different clusters. The similarity percentage (SIMPER) routine of the PRIMER v6 software (Clarke and Gorley, 2006) was used to identify the key taxa that characterized those clusters. Characterizing taxa were defined as those taxa that contributed N 5% to cluster similarity. The relationships between faunal assemblages and the examined ground floor variables (seafloor type, depth and slope) were investigated using the BIO-ENV procedure in the PRIMER v6 software, to determine which environmental condition best explained the distribution of taxa. Information about seafloor type was superimposed over the non-metric multidimensional scaling plot (nMDS) to visually investigate the relationship between substrate characteristics and faunal assemblages.

3.2.2. Sediment samples

Grab samples were collected at 17 stations (Fig. 2) using a 30 L Van Veen Grab. All materials collected (except for station 26) were subsampled using a ~10 cm long core to obtain relatively undisturbed samples. Samples from the top (T) and bottom (B) of the cores, and eventually

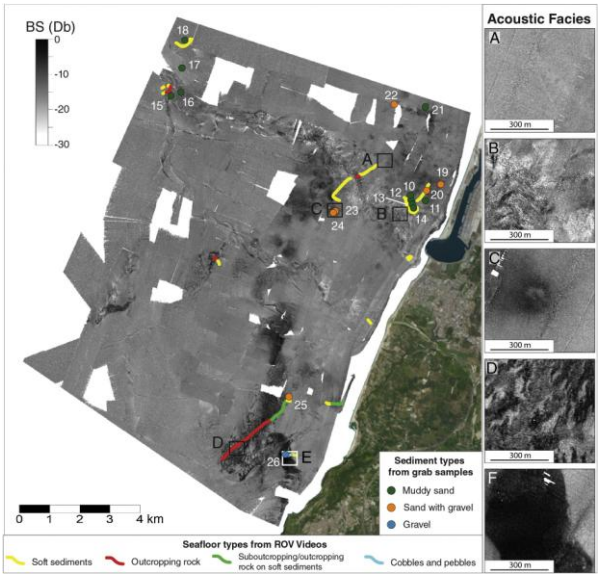

Fig. 3. Backscatter map and acoustic facies from the study area. The lines overlying the backscatter map represent the ROV transects, with the different colors referring to the seafloor classes defined from the video analysis. Symbols represent the classes of sediment types derived from the analysis of grab samples. The location of the acoustic facies illustrated in the insets on the right is denoted by the black boxes.

Table 1
Location and water depth of video transects collected with the ROV Pollux III.

Transect	Cruise	Date	Transect location	Length	Position				Depth
				(m)	Start		End		(m, start–end)
T_1	Tygraf	17/02/2013	Gioia Canyon	657	38°27.74′N,	15°53.45′E	38°27.45′N,	15°53.21′E	65–118
T_3	Tygraf	22/02/2013	Gioia Canyon	875	38°27.51′N,	15°52.99′E	38°27.35′N,	15°53.22′E	105–154
T_4a	Tygraf	22/02/2013	Gioia Canyon	122	38°28.10′N,	15°52.26′E	38°27.91′N,	15°51.86′E	121–300
T_4b	Tygraf	22/02/2013	Gioia Canyon	1137	38°27.87′N,	15°51.68′E	38°27.48′N,	15°51.43′E	274–141
T_5	Tygraf	23/02/2013	Shelf break	231	38°22.92′N,	15°50.34′E	38°22.91′N,	15°50.19′E	115–146
T_6	Tygraf	23/02/2013	Palmi Ridge	850	38°23.89′N,	15°50.23′E	38°23.61′N,	15°49.92′E	86–101
T_6bis	Tygraf	23/02/2013	Palmi Ridge	351	38°23.61′N,	15°49.94′E	38°23.53′N,	15°49.77′E	99–120
T_7	Tygraf	24/02/2013	Inner shelf	461	38°23.84′N,	15°51.43′E	38°23.84′N,	15°51.12′E	40–64
T_8	Tygraf	25/02/2013	Palmi Ridge	2126	38°23.53′N,	15°49.79′E	38°22.86′N,	15°48.69′E	116–389
T_9	Tygraf	25/02/2013	Upper slope	110	38°26.42′N,	15°48.62′E	38°26.45′N,	15°48.56′E	265–281
T_10	Tygraf	26/02/2013	Upper slope	565	38°30.41′N,	15°48.05′E	38°30.31′N,	15°47.77′E	404–408
T_11	Tygraf	26/02/2013	Gioia–Petrace confluence	110	38°29.56′N,	15°47.45′E	38°29.56′N,	15°47.51′E	465–449
M_1	Magic-0112	09/01/2012	Gioia Canyon	610	38°26.46′N,	15°53.05′E	38°26.42′N,	15°53.04′E	86–79
M_2	Magic-0112	09/01/2012	Petrace Canyon	102	38°25.27′N,	15°52.10′E	38°25.30′N,	15°52.08′E	43–54

Table 2
Location ,water depth and granulometric characteristics of grab samples collected during Tygraf cruise.

Station	Date	Sample location	Position		Depth (m)	Sub-sample	%Gravel	%Sand	%Silt	%Clay	D50 (mm)	Cluster
10	22/02/2013	Gioia Canyon margin	38°27.53′N,	15°52.99′E	−106	10_T	0.16	37.71	49.1	13.03	0.037	A
						10_B	0.17	47.65	40.03	12.15	0.056	A
11	22/02/2013	Gioia Canyon margin	38°27.46′N,	15°53.48′E	−101	11_T	0.44	32.1	54.68	12.78	0.035	A
						11_B	1.45	47.54	40.07	10.94	0.06	A
12	22/02/2013	Gioia Canyon flank	38°27.44′N,	15°53.01′E	−130	12_T	0.14	32.72	53.9	13.24	0.033	A
						12_B	0.79	41.84	44.19	13.18	0.045	A
13	22/02/2013	Gioia Canyon flank	38°27.35′N,	15°53.04′E	−161	13_T	0.02	20.2	60.19	19.59	0.018	A
						13_S	2.89	78.56	14.46	4.09	0.376	B
						13_B	0.02	31.62	53.43	14.93	0.032	A
14	22/02/2013	Gioia Canyon thalweg	38°27.28′N,	15°53.07′E	−197	14_T	0.04	35.53	50.94	13.49	0.035	A
						14_B	0	35.09	50.66	14.25	0.036	A
15	26/02/2013	Petrace Canyon thalweg	38°29.43′N,	15°47.54′E	−503	15_T	0.04	54.25	35.6	10.11	0.068	A
						15_B	0.03	76.91	18.03	5.03	0.092	A
16	26/02/2013	Gioia Canyon thalweg	38°29.46′N,	15°47.70′E	−543	16_T	0.02	31.47	54.17	14.34	0.033	A
						16_B	0.01	59.83	31.61	8.55	0.077	A
17	26/02/2013	Gioia Canyon margin	38°29.94′N,	15°47.79′E	−388	17_T	0	20.32	61.32	18.36	0.022	A
						17_B	0	20.7	62.45	16.85	0.023	A
18	26/02/2013	Upper slope	38°30.38′N,	15°47.96′E	−403	18_T	0	17.56	63.62	18.82	0.02	A
						18_B	0	17.91	62.48	19.61	0.018	A
19	27/02/2013	Inner shelf	38°27.90′N,	15°53.86′E	−63	19_T	1.31	81.77	13.82	3.1	0.195	B
						19_S	2.32	84.66	10.67	2.35	0.24	B
						19_B	0.38	81.86	14.26	3.5	0.187	B
20	27/02/2013	Gioia Canyon margin	38°27.63′N,	15°53.40′E	−92	20_T	3.68	57.72	32.36	6.24	0.087	B
						20_B	11.71	66.31	17.37	4.61	0.532	B
21	27/02/2013	Outer shelf	38°29.20′N,	15°53.43′E	−101	21_T	0.23	31.25	55.71	12.81	0.033	A
						21_B	3.89	44.44	42.11	9.56	0.059	A
22	27/02/2013	Outer shelf	38°29.21′N,	15°52.78′E	−104	22_T	11.46	58.85	23.75	5.94	0.371	B
						22_B	25.26	54.23	16.57	3.94	1.07	B
23	27/02/2013	Outer shelf	38°27.32′N,	15°51.36′E	−129	23_T	7.66	49.87	34.37	8.1	0.078	B
						23_B	0.74	33.72	50.94	14.6	0.033	A
24	27/02/2013	Outer shelf	38°27.30′N,	15° 51.30′E	−129	24_T	13.34	63.49	18.66	4.51	0.189	B
						24_B	0.58	37.49	49.18	12.75	0.041	A
25	27/02/2013	Outer shelf	38°23.92′N,	15°50.17′E	−80	25_T	1.96	80.16	14.18	3.7	0.133	B
						25_B	1.37	71.71	20.8	6.12	0.116	B
26	27/02/2013	Upper slope	38°22.91′N,	15°50.15′E	−164	26	65.59	26.21	6.21	1.99	5.743	C

intermediate layers (S), were taken for grain size analysis, which generated 35 sub-samples (Table 2). Dry sieving at one-phi intervals was carried out for the fraction coarser than 62 μm. The finer fraction was analyzed using a Sympatec laser system at one-quarter phi intervals. The final grain size distribution was obtained by proportional recombination of the individual data sets.

3.2.2.1. Statistical analyses on sediment samples. The particle size distribution for sediment samples was examined using multivariate statistical procedures with the software PRIMER v6 (Clarke and Gorley, 2006). A hierarchical cluster analysis was performed over the square root-transformed particle size dataset, selecting the Euclidean distance similarity measure and the average linkage cluster analysis algorithm. The result is presented in the form of a dendrogram and a non-metric multi-dimensional scaling (nMDS) ordination plot, both used to classify sampling stations into categories of sediment types.

3.3. Acoustic seafloor classification and analyses of backscatter data

The backscatter map was segmented into a discrete number of acoustic facies following an unsupervised approach based on the expert judgement of a single observer to identify areas of similar backscatter intensity and pattern (i.e. van Rein et al., 2011). Acoustic facies were related to different seafloor characteristics by comparison of backscatter values with classification from grab sample analyses and ROV images, to obtain the acoustic seafloor classification. The relationships between backscatter intensity and seafloor composition were examined through one-way permutational multivariate analysis of variance (PERMANOVA; Clarke and Gorley, 2006). The PERMANOVA pairwise post hoc test was used to test the significance of differences in mean backscatter intensity associated with distinct seafloor classes that were derived from the analysis of groundtruth data (see Section 3.2).

4. Results

4.1. Geomorphology

4.1.1. Continental shelf

Bathymetric data show that the continental shelf is very narrow (3 to 4 km wide) and steep (1°–2°), becoming completely absent south of the Palmi promontory (Fig. 1). The shelf break is located at an average depth of 130–140 m.

The inner shelf (between 5 and 50 m depth) is characterized by the presence of a sedimentary wedge, which runs parallel to the coastline (Fig. 2A and Fig. 4). This sedimentary wedge has a flat top, with variable width (80–450 m), developing down to 12–25 m depth. A steep frontal slope with gradients up 20° (Fig. 2B) connects the wedge with the middle shelf.

The Gioia–Mesima canyon system represents the most prominent morphological feature of the continental shelf. Bedform fields and small-scale incisions (gullies) (Fig. 4), occur in the northern part of the study area. The bedform fields have a general lobate or fan shape, elongated sub parallel to the main slope direction (Fig. 4). Most bedforms (50 to 120 cm high with average wavelength of 40 m) are cut by a network of small gullies (50 to 100 cm deep), some of which are tributaries of the Gioia and Petrace canyons (Fig. 4). At Palmi Ridge, shelf areas are characterized by a rough morphology due to the presence of outcropping and sub-outcropping rocks (Fig. 5). Here, at the foot of the sedimentary wedge (about 50 m depth) comet marks have formed in association with small rocky outcrops (1 to 10 m high and up to 40 m wide, Fig. 5) and suggest the action of bottom currents flowing northward parallel to the coastline.

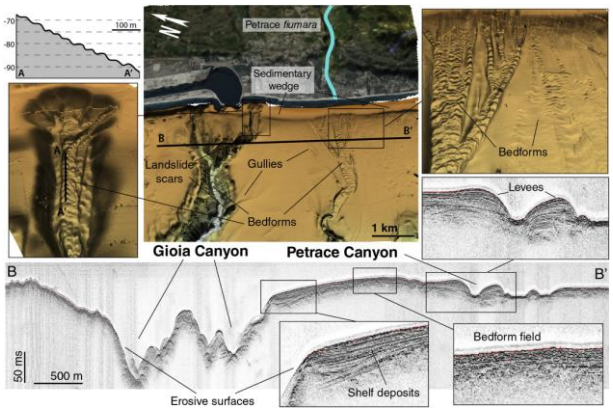

Fig. 4. 3-D view of the Gioia and Petrace Canyon heads showing the main geomorphological features along this sector. The seismic profile parallel to the coastline shows the different incision produced by the two canyons and the presence of levees at the Petrace Canyon margins.

4.1.2. Continental slope

The continental slope gently dips toward the Gioia basin with an average gradient of 2.7° (Fig. 2B). The smooth morphology of the slope is interrupted by the Gioia and Petrace canyon system and by a series of escarpments (on average 10° to 15°steep) mostly oriented NE−SW (Fig. 2A and B). The most prominent escarpment is the Palmi Ridge, (Fig. 5) which produces a wide bulge along the outer shelf and upper slope down to 400 m depth. South of the Palmi Ridge the continental shelf is absent and the costal sector is directly connected to the Palmi Basin (−400 m) through a steep escarpment with gradients up to 35° (Fig. 2B).

4.1.3. Gioia and Petrace canyon system

The Gioia and Petrace canyons are oriented SE-NW and run parallel for about 8 km across the continental shelf and the upper part of the continental slope (Fig. 2 and Fig. 4). At about 350 m depth the Petrace Canyon bends toward the north, developing a series of meanders before merging with the Gioia Canyon at about 450 m depth (Fig. 2).

The Gioia Canyon head has two branches (Fig. 4). The northern and southern branches deeply indent the sedimentary wedge up to very shallow depths of about 8-10 m, at distances from the coastline of only 80 and 100 m respectively. They merge into a single course at around 100 m depth. The canyon is about 1 km wide, exhibiting a V shaped profile and erosive flanks that are characterized by numerous instability features, such as landslide scars and gullies (Fig. 4). The relief of the canyon flanks increases with depth from about 50 m at the canyon head to more than 200 m at the shelf break and along the upper slope. The thalweg is about 100 m wide and floored by crescent shaped bedforms 3 to 6 m high, with wavelengths ranging from 30 to 150 m (Fig. 4). The height and wavelength of these bedforms increase with depth. Their shape is asymmetric downslope, with a sub-horizontal stoss side and a steep lee side.

The head of the Petrace Canyon is located at the mouth of the Petrace fiumara (Fig. 4), where the edge of the sedimentary wedge is breached by multiple gullies up to a depth of 15 m. These gullies are incised 5 to 10 m and merge into three main branches that finally join together at 100 m depth.

The Petrace Canyon is less than 500 m wide and has smooth flanks about 20 m high (Fig. 4). The height of the flank increases up to 50 m at the shelf break and close to the confluence with the Gioia Canyon, where some landslide scars are present at the canyon margins. The thalweg is about 150-250 m wide and exhibits crescent shaped bedforms on the floor (Fig. 4), whose dimensions are similar to those observed along the thalweg of the Gioia Canyon.

4.2. Seismic facies

The chirp profile along the continental shelf shows the presence of a stratified seismic facies, with sub-horizontal parallel reflectors characterized by medium-high amplitude and medium lateral continuity (Fig.4). The bedform field areas are associated with a stratified seismic facies characterized by discontinuous internal reflectors (Fig. 4). These shelf deposits represent post-glacial deposits, as they overlay an erosional surface (LGM unconformity, Fig. 5) that correlates with a regional unconformity depicted on the Calabrian margins as well as on the Italian shelves, referred to the last low-stand of sea level (Chiocci et al., 1989; Martorelli et al., 2014). In the southernmost sector of the study area,

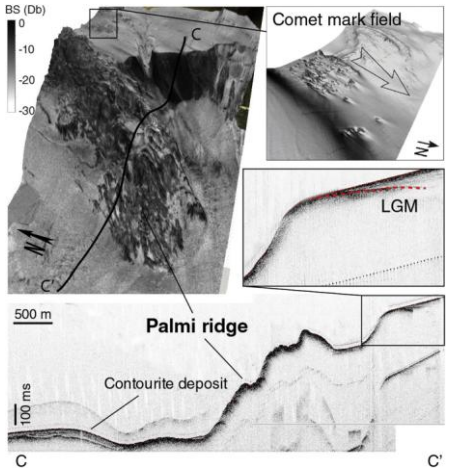

Fig. 5. Backscatter map overlapped on the 3D view of the Palmi Ridge. The image illustrates the dishomogeneous pattern of backscatter intensity associated with the ridge and the very high backscatter facies in correspondence of the steep slope south of the ridge. The seismic profile shows the LGM unconformity outcropping in proximity of the shelf break, the deaf seismic facies in correspondence with the Palmi Ridge, and the presence of contourite deposits at its foot.

where the width of the continental shelf is very restricted (1.5 to 0.6 km), the LGM unconformity outcrops in proximity of the shelf break and along the uppermost part of the slope (Fig. 5).

Erosional surfaces (usually characterized by truncated internal reflectors or high-amplitude reflectors with no sub-bottom echoes) are present along the flank of the Gioia Canyon (Fig. 4), together with hyperbolic echoes of variable height. Slightly asymmetric levees are present at the Petrace Canyon margins (Fig. 4), from the canyon head down to the middle shelf (about −100 m).

The chirp profile along the continental slope shows the dominance of an undisturbed seismic stratified facies, with medium amplitude and high lateral continuity, whereas a high reflective seismic facies with no sub-bottom echo was observed corresponding to the rocky outcrops of the Palmi Ridge and the slope escarpments (Fig. 5). The seismic profile crossing some mound-shaped bodies, observed on the bathymetry between 250 and 350 m depth, also evidenced the presence of a stratified facies, whose internal reflector geometry is interpreted here to be related to contourite deposits (Fig.5).

4.3. Seafloor types determined from ROV images

Four seafloor types were visually identified from the 14 video transects: soft sediment, sub-outcropping and outcropping rocks on soft sediment, outcropping rocks, and cobbles and pebbles. Their distribution is shown in Fig. 3.

Soft sediment (Fig. 6) is the predominant seafloor type observed in the study area. It is widely distributed both inside and outside of the Gioia and Petrace canyons (Fig. 3). Bioturbated soft bottoms are locally present within the Gioia Canyon head, along the canyon margins, in the thalweg, and on the gently sloping sectors of the canyon flanks. Soft sediments also characterize shelf and slope areas adjacent to the canyon.

Sub-outcropping and outcropping rocks on soft sediment (Fig. 6) occur in the southern sector of the study area, in the comet mark field, and at the shelf break along the Palmi Ridge (Fig. 3). Outcropping rocks (Fig. 6) are locally present along the flanks of the Gioia Canyon, preferentially observed on the lower and steeper part of the canyon flanks (Fig. 3). At the confluence of the Gioia and Petrace canyons at 400 m depth, landslide blocks at the base of the canyon flanks are also present. Outside the canyon, rocky outcrops occur on the Palmi Ridge and the steep escarpments of the upper slope (Fig. 3).

A seabed characterized by rounded cobbles and pebbles (Fig. 6) is observed in the southernmost sector of the study area, south of the Palmi Ridge. Cobbles and pebbles distribute along the shelf break and the upper continental slope (Fig. 3), starting at depths of about 120 m.

4.4. Surficial sediment characteristics

Based on grain size analyses and multivariate statistics on grab samples three different types of sediments can be distinguished within the study area: muddy fine sand, muddy fine sand with gravel and gravelly sediment (Fig.7A and C). Their spatial distribution is shown in Fig. 3.

The majority of the samples are included in Cluster A and are characterized by a silty-fine sand composition (Fig. 7B). These sediments are mainly distributed around the canyon head, in the thalweg, and on the upper part of the continental slope (Fig. 3). The samples from the

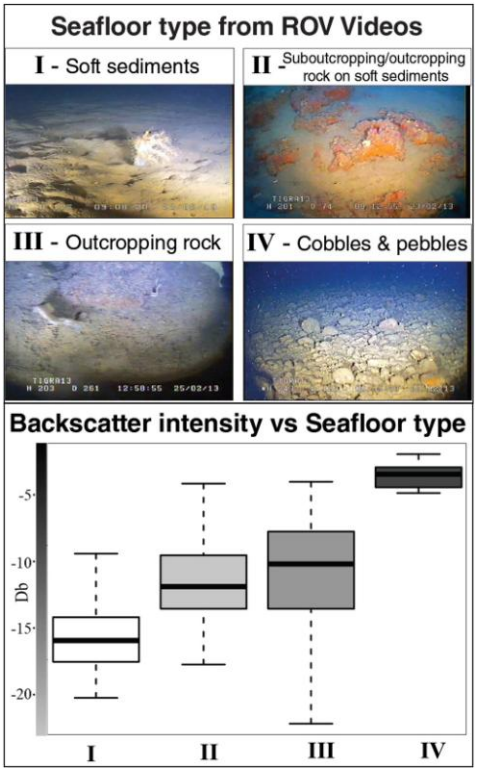

Fig. 6. Seafloor types derived from the analysis of the ROV videos. The box plots on the bottom show the backscatter intensity pertaining to each classified seafloor type. I – Soft sediments; II – Sub-outcropping/outcropping rock on soft sediments; III – Outcropping rock; IV – Cobble and pebbles.

continental slope show the highest percentage of mud (80%), while the sandy/muddy fraction is on average around 40%–60% for all the other samples (Table 2). In some cases, the bottom layers of the samples had a slightly larger sand fraction. This is particularly true for stations 15 and 16, located in the thalweg of the Gioia and Petrace canyons at 500 m depth, in which the bottom sub-samples (B) are largely (75%) composed of sand.

The sub-samples of Cluster B are characterized by the presence of a coarser fraction along with the fine component (Fig.7B). These samples are very poorly sorted with a bimodal size distribution. The percentage of gravel varied between 2% and 25%, and the muddy fraction is on average around 20%–25% (Table 2). This type of sediment occurs on the continental shelf located in the northern part of the Gioia Canyon head, at the shelf break between the Gioia and Petrace Canyon and on the outer shelf, on the Palmi Ridge (Fig. 3). The gravel fraction is generally dominated by rounded lithoclasts, with the exception of station 25 which is characterized by broken bivalve and gastropod shells and bryozoan fragments.

Cluster C includes only station 26, collected on the upper slope south of the Palmi Ridge (Fig. 3). Its sediment is composed of small amounts of sand, gravel and centimetric pebbles (Fig. 7B).

The top (T) and the bottom (B) sub-samples from each station show a rather similar grain size distribution, belonging to the same cluster. In contrast, stations 23 and 24 are characterized by top sub-samples composed by coarse-grained sands and gravels mixed with fine sediments (Cluster B) while bottom sub-samples are composed of muddy fine sands (Cluster A).

4.5. Backscatter distribution and acoustic seabed classification

From the analysis of the backscatter intensity and pattern it is possible to distinguish 5 different acoustic facies occurring in the study area (Fig. 3).

Acoustic facies A (Fig. 3A) corresponds to a homogenous low backscatter facies (from −15 to −20 db) and is located primarily along the slope and a large part of the continental shelf. In contrast, acoustic facies B (Fig. 3B) is defined by a non-homogeneous backscatter pattern (from very low backscatter values of −25 db to high backscatter values of −5 db) and is mainly distributed along the Gioia and Petrace canyon areas.

Acoustic facies C (Fig. 3C) corresponds to the medium and high backscatter patches (from −14 to −10 db) and is locally distributed along the shelf sector north of the Gioia Canyon head and along the canyon margins and the shelf break between the Gioia and Petrace canyons, where the backscatter anomalies often exhibit a distinctive "ring-like" shape.

Acoustic facies D (N −13 db, Fig. 3D) is characterized by high backscatter intensities interrupted by low backscatter patches and is observed in correspondence with the comet mark field and along the upper continental slope of the southern sector, primarily associated with the rocky outcrops of the Palmi Ridge.

Acoustic facies E (Fig. 3E) corresponds to very high and homogenous backscatter intensity (N −5 db,) and is observed along the upper continental slope south of the Palmi Ridge.

The integration of acoustic facies with the seafloor types derived from the ROV images (see Section 4.3) and sediment types derived from grabs (see Section 4.4) shows a positive relationship between backscatter intensity and seafloor grain size, with coarsest sediment and rocky outcrops having the highest intensities (Figs. 6 and 7D). In particular, acoustic facies A is associated with the seafloor type "soft sediments" determined from ROV observations (I in Fig. 6) and with the muddy fine sand samples (Cluster A). Acoustic facies B with heterogeneous backscatter intensities is associated with "soft sediments" and "outcropping rock" (I and III in Fig. 6). Acoustic facies C is associated with "soft sediments" and with muddy fine sands with gravels (Cluster B). Acoustic facies D is related to the different rocky classes determined from the ROV images (II and III in Fig. 6). Acoustic facies E is related to "cobbles and pebbles" (IV in Fig. 6) and with gravelly sediment (Cluster C).

The PERMANOVA pairwise post hoc test (Table 3) confirms the significant relationship between seafloor types derived from the ROV images and the backscatter intensity exhibited by the different acoustic facies ($p < 0.01$). The resulting map of distribution of the seafloor types is illustrated in Fig. 8A. The seafloor type "sub-outcropping and outcropping rocks on soft sediment" and "outcropping rock" (II and III in Fig.6) resulted in no statistically different classes in the PERMANOVA analysis (Table 3). Hence they are grouped as one unique class in the final seafloor map: sub-outcropping and outcropping rock (Fig. 8A). The slope gradient has been adopted as a surrogate to map the distribution of outcropping rock within the canyons, with values over 30° representing rocky areas.

4.6. Megabenthic communities

A total of 89 sampling units were used for the statistical analyses. The video sequences covered a linear distance of 4.45 km across a wide range of slopes, substrates and depths. A total of 41 invertebrate and 12 fish taxa (including all taxonomic and morphotype levels) were identified in the analyzed footage (Appendix A). The cluster

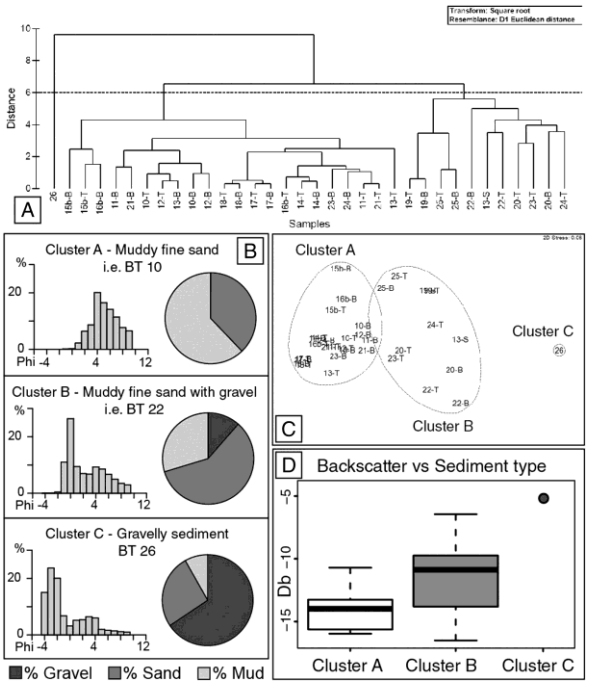

Fig. 7. A: Dendrogram of hierarchical cluster analysis of grain size data from grab samples. B: Examples of grain size distribution and gravel/sand/mud weight proportion for each of the three clusters identified. C: Two-dimensional ordination plot from non-metric multidimensional scaling of grain size data. The samples are grouped according to the three cluster identified. D: Box plots showing the backscatter intensity pertaining to each cluster of sediment type. Backscatter intensity pertaining to Cluster C, that features only one sample, is indicated by the gray dot.

analysis and the SIMPROF routine identified five significantly different benthic assemblages (Fig. 9). These five assemblages are reasonably well defined in terms of taxa composition ($p < 0.01$) with a mean within-assemblage similarity (based on Bray–Curtis distances of square root transformed data) between 35% and 61%.

Assemblage 1 is largely dominated by the sea pen Pennatula rubra (Fig. 10A) and a Sabellid polychaete that could not be identified to species level. These two taxa co-occurred with the sea pen Funiculina quadrangularis (Fig. 10D) and the crinoid Leptometra phalangium (Fig. 10B). Other less common species also observed in Assemblage 1 are the soft-coral Alcyonium palmatum, the cerianthid Andresia parthenopea and a pedunculated sponge identified as Rhizaxinella pyrifera. This assemblage mostly occurs over soft sediments and is distributed over the canyon head and margins, as well as on the adjacent shelf (Fig. 9). Most of the characteristic species of this assemblage, primarily P. rubra, Sabellidae and L. phalangium, are distributed at a depth range between 80 and 260–280 m. By contrast, F. quadrangularis is found in deeper areas starting from 130 m, down to 450 m depth.

Table 3
PERMANOVA pairwise post hoc test results (unshaded) and average distance between seafloor types based on Euclidean distance of untransformed backscatter intensity values (shaded).

Seafloor type	I	II	III	IV
I		**	**	**
II	4.56		*	**
III	5.89	4.30		**
IV	11.63	7.87	7.33	

I — Soft sediments; II — Sub-outcropping/outcropping rock on soft sediments; III — Outcropping rock; IV — Cobble and pebbles.
* $p < 0.01$.
** $p < 0.01$.

Assemblage 2 is characterized by an abundant taxon of shrimp, a cerianthid and some polychaetes, which constituted the dominant groups. This assemblage is distributed on the canyon flanks (Fig. 9) between 200 and 500 m depth, both in areas of soft sediments and sub-outcropping and outcropping rocks. In this last case, shrimps and cerianthids largely dominated the assemblage, while polychaetes are only present when there is a thin veneer of sediment over the rocks.

Assemblage 3 featured the octocorals Isidella elongata (Fig. 10H), Kophobelemnon stelliferum and F. quadrangularis (Fig. 10D) as the most common species. This assemblage was only present on the canyon margins and flanks at the confluence between the Gioia and Petrace canyons, at about 450 m depth (Fig. 9). I. elongata is distributed on the

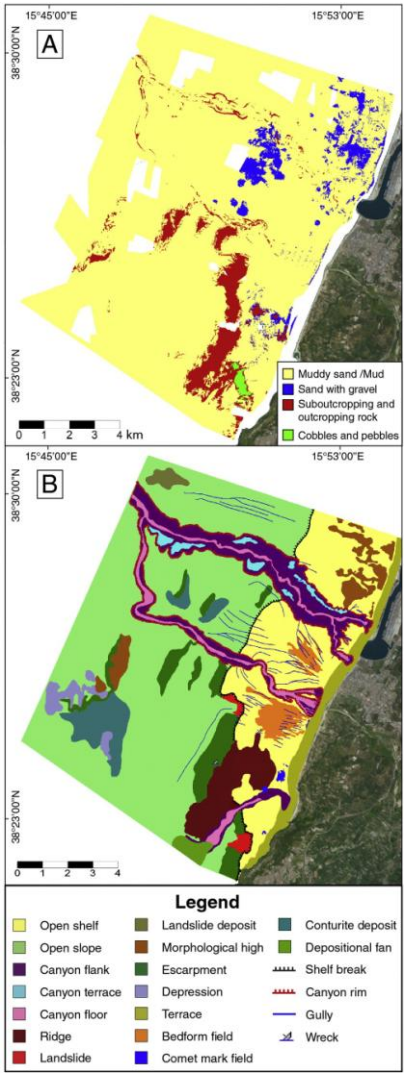

Fig. 8. Sediment (A) and geomorphological map (B) derived from the analysis of multibeam data.

soft sediments of the margins and also on the semilithified mudstones that outcrop on the upper part of the flanks. K. stelliferum and F. quadrangularis are observed mostly at the Gioia Canyon margins or where a local accumulation of fine sediment along the flanks is present.

Assemblage 4 is characterized by wide occurrence of the black coral Antipathella subpinnata (Fig. 10G), along with the echiurid Bonellia viridis, the sea urchin Centrostephanus longispinus and various species of sea stars. Other species observed included a variety of sponges and polychaetes. This assemblage is also characteristic of hard substrates and only observed on sub-outcropping and outcropping rocks on soft sediments in different areas of the shelf break (80–130 m depth) in association with the Palmi Ridge (Fig. 9). Soft bottoms in this area are colonized by Assemblage 1, whose composition differed slightly from its counterpart in the canyon area. The occurrence of monospecific patches of the hydroid Lytocarpia myriophyllum (Fig. 10C) is observed on soft bottoms around the Palmi Ridge in the ROV footage. On the contrary, the rocky outcrops are colonized by large colonies of A. subpinnata that hosted a very rich associated community, with most species too small to identify, and hence not included in the statistical analyses.

The most abundant and most frequent species of Assemblage 5 are the sea urchin Cidaris cidaris (Fig. 10F) and the sponge Pachastrella monilifera (Fig. 10I). Other taxa observed in this cluster include the polychaete Protula sp. (Fig. 10E), the sponge Poecillastra compressa and some holothurians. Assemblage 5 is mainly present over hard substrates of the upper slope, outside the canyon (Fig. 9). It occurs along the Palmi Ridge from just below the shelf break down to 400 m depth and on the rocky escarpment along the continental slope in the southern sector of the study area.

Regarding the fish fauna, the most common species observed in the canyon were Helicolenus dactylopterus and Coelorinchus caeolorhincus, which were also present in association with rocky bottoms of the slope escarpments and around the Palmi Ridge. In these areas, shoals of Trachurus trachurus could be observed at depths of about 300 m. Other species identified in the canyon transects were Merluccius merluccius, Capros aper and Peristedion cataphractum.

4.7. Relationships between faunal assemblages and seafloor characteristics

The results from the BIO-ENV procedure (Table 4) show that the most important seafloor variable determining the distribution of the different taxa was seafloor type ($\rho = 0.547$). Correlation values obtained combining the rest of the variables were slightly weaker and a larger decline was observed when seafloor type was not included.

The MDS plot (Fig. 11) indicates that the greatest difference in taxa composition can be found between the assemblages associated with soft bottoms and those colonizing hard substrates. A further differentiation in the composition of the benthic communities is observed when comparing areas inside and outside the Gioia Canyon.

4.8. Anthropogenic alterations of the seabed

A diffuse anthropogenic alteration of the seafloor is revealed by ROV observations, showing several deep tracks on the seafloor caused by trawling gear (Fig. 12A, B and C). Trawl marks are present on the soft bottoms in many surveyed stations, except for the steepest part of the canyon walls and the thalweg. Along the continental slope adjacent to the Gioia Canyon (ROV T11, Fig. 2), large areas of the seafloor show evidence of repeated trawling, which smoothes and ploughs the seabed. Furthermore, several lost fishing lines (Fig. 12D) are observed on the rocky bottoms of the Palmi Ridge.

A remarkable quantity of litter including plastic bags, tires, bottles and pieces of wood is present within the thalweg area of the Gioia and Petrace Canyon (Fig. 12E and F).

A further possible human-induced alteration of the seabed is suggested by the high backscatter areas showing a distinctive "ring-like" structure, that were observed at the shelf break and along the canyon

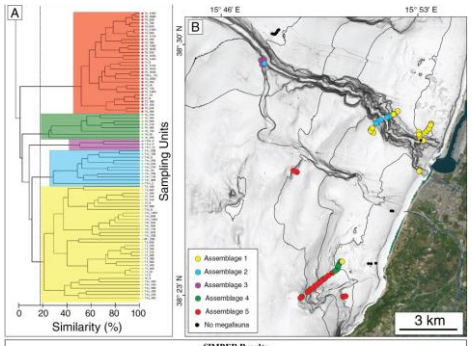

SIMPER Results				
Assemblage 1	Assemblage 2	Assemblage 3	Assemblage 4	Assemblage 5
Pennatula rubra	Shrimp sp1	*Kophobelemnon stelliferum*	*Antipatella subpinnata*	*Cidaris cidaris*
Sabellidae	*Cerianthus* sp.	*Isidella elongata*	*Bonellia viridis*	*Pachastrella monilifera*
Funiculina quadrangularis	Sabellidae	*Funiculina quadrangularis*	*Centrostephanus longispinus*	
Leptometra phalangium			Asteroidea sp 1	
Lytocarpia myriophyllum				

Fig. 9. A: Dendrogram of hierarchical cluster analysis of species data. The colored box indicates the megafaunal assemblages and colors refer to the legend in B. B: Bathymetric map showing the spatial distribution of the identified assemblages. Characteristic species for each assemblage resulting from SIMPER analysis are indicated in the boxes on the bottom.

margins (Fig. 13). These features were likely created by the disposal of material from dredging operations. Indeed, similar structures have been observed in known areas where disposal of dredge spoil has occurred, on the Pacific and Atlantic continental shelves (Poppe et al., 2001; Galparsoro et al., 2010). The grain size analyses on the sediment samples collected near the "ring-like" structures (stations 23 and 24, Fig. 3) had top (T) sub-samples with coarse-grained sand and gravel mixed with fine sediments (Cluster B: poorly sorted sediments), while better sorted muddy fine sands without the coarse-grained fraction were present in bottom subsamples, away from the spoil dump sites (Cluster A).

5. Discussion

5.1. Active geomorphic features

Our analyses of the Gioia and Petrace canyons show that they are characterized by several morphosedimentary features (i.e. crescent-shaped bedforms, gullies...) indicative of vigorous sediment transport processes, consistent with previous observations (Colantoni et al., 1992; Gamberi and Marani, 2008).

From the multibeam data, bedload sediment transport within the Gioia and Petrace canyons is shown by the crescent-shaped bedforms observed along their thalwegs. These are similar to the bedforms interpreted as cyclic steps and attributed to the action of turbidity flows (Cartigny et al., 2011) that have been observed in active canyons: e.g. the Monterey Canyon (Paull et al., 2010b), the Nazaré Canyon (Masson et al., 2011) and the Eel Canyon (Lamb et al., 2008). The downslope asymmetry of the cyclic steps observed within the thalweg of Gioia and Petrace canyons is characteristic of high-energy confined settings (Cartigny et al., 2011). This setting would encompass erosional flows, as evidenced by eroded strata exposed at the base of the canyon's flanks, observed on the ROV videos at the Gioia and Petrace heads. Therefore, these bedforms are interpreted here as indicating very recent sedimentary activity of the Petrace and Gioia canyons in their upper reaches (b 250 m). On the upper reach of the Petrace Canyon, bathymetric and seismic data also indicated that turbidity currents were able to overspill the canyon walls, forming well-developed levees.

As shown by bathymetric data, both the Gioia and Petrace canyons indent the shelf up to very shallow water depth (8–10 m Gioia and 12 m Petrace), eroding the infra-littoral sedimentary wedge in relation to the retrogressive evolution of their heads. Due to the very shallow setting and the proximity with the mouth of the Petrace fiumara, it is likely that turbidite flows are originated by sediments delivered both by longshore currents and by the nearby fiumara. Given this very shallow canyon origin, the littoral drift, flowing both in a northern and southern direction and converging into the Gioia Canyon head (Lupia Palmieri et al., 1997), should provide a significant contribution to the canyon activity. Further evidence of funneling of coastal sediment into the Gioia Canyon was provided by Colantoni et al. (1992), who observed

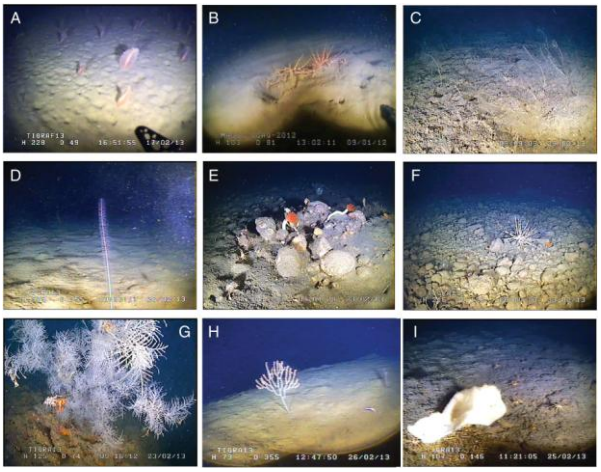

Fig. 10. Selected ROV images of the megafauna observed in the Gulf of Gioia. A: the sea pen Pennatula rubra (50 m depth); B: the crinoid Leptometra phalangium (80 m depth); C: colonies of the hydroid Lytocarpia myriophyllum (75 m depth); D: the sea pen Funiculina quadrangularis (350 m depth); E: the polichaete Protula sp. (115 m depth); F: the sea urchin Cidaris cidaris (120 m depth); G: colony of the black coral Antipathella subpinnata (75 m depth); H: colony of the octocoral Isidella elongata (350 m depth); I: the deep-sea sponge cf. Pachastrella monilifera (145 m depth).

that the sediment accumulated at the canyon head is deposited on slopes that are close to the critical angle of repose. It is therefore likely that perturbations such as storm-waves or earthquakes trigger failures

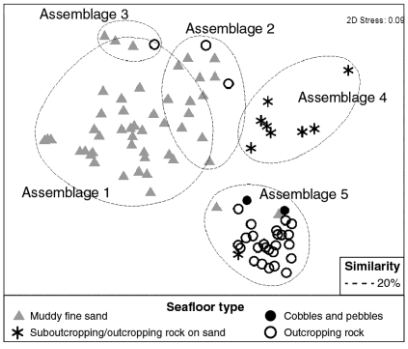

Fig. 11. Two-dimensional ordination plot from non-metric multidimensional scaling of species data. Sampling units are grouped according to the assemblages resulting from the cluster analysis. The symbols refer to the seafloor type associated to each sampling unit.

and gravity flows within the canyon. The coastal retreat observed within the last 50 years in this area has been attributed to the funneling of coastal sediments into the canyon (D'Alessandro et al., 2002). Furthermore, like most of the Calabrian river courses, the Petrace fiumara is characterized by torrential inputs of floodwaters, vegetal detritus, debris and suspended organic matter, strictly related to the seasonal rainfalls, that are supplied to the shelf and canyons. Catastrophic flash floods can occur with a recurrence period of a few years (Sabato and Tropeano, 2004). The high discharges during major floods, which can be up to several hundreds of m^3/s (Sorriso-Valvo and Terranova, 2006), are likely to promote the development of turbidity currents within the canyons (e.g. Casalbore et al., 2011).

The redistribution of littoral deposits during sea storm events, high fiumare discharges and erosion of the infra-littoral sedimentary wedge

Table 4
Results obtained with the BIO-ENV analysis, showing the combinations of the ground floor and depth variables, taken k at time, and the corresponding Spearman coefficient (ρ).

BIO-ENV comparison		
k	Ground floor and depth variables	(ρ)
1	Seafloor type	0.547
1	Slope	0.409
1	Depth	0.251
2	Seafloor type, depth	0.545
2	Seafloor type, slope	0.538
2	Depth, slope	0.417
3	Seafloor type, depth, slope	0.545

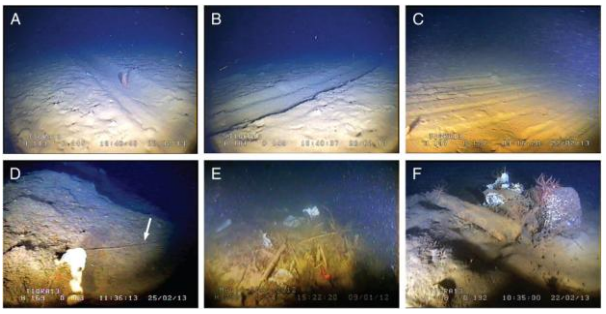

Fig. 12. ROV images showing impact of human activities on the seafloor in the study area: trawl marks over soft bottoms (A, B, C), fishing lines (D) and littering within the thalweg of the Petrace (E) and Gioia (F) canyons.

can explain also the sedimentological heterogeneity that was observed along shelf sectors adjacent to the Gioia Canyon, as well as the widespread distribution of morphosedimentary features indicating sediment transport (i.e. bedform field and gullies) outside the canyon areas.

As a whole these results suggest that cross-shore sediment transport processes may affect most of the continental shelf environment in this sector of the Calabro–Tyrrhenian margin. Here, high amount of postglacial deposits accumulated on the continental shelf, forming a 60–70 m thick sedimentary wedge (Colantoni et al., 1992), which is among the thickest shelf deposit observed along the Tyrrhenian margin. This reflects high sedimentation rates, favored by high uplift rates and fault activity along the mainland during Quaternary times, which produce denudation rates exceeding 800 mm/ka (Critelli and Le Pera, 1998).

A very different scenario is that of the Palmi Ridge where fluvial supply is absent and stronger hydrodynamism occurs. Here, the seabed of the continental shelf and slope alternates between smooth areas dominated by sediment to rough areas with rocky outcrops, creating a more varied seafloor composition. Large rocky outcrops of the Palmi Ridge reflect the local tectonic setting, producing a steep escarpment on the outer-shelf /upper continental slope sector oriented along a main NE–SW fault system (Fabbri et al., 1980; Barone et al., 1982).

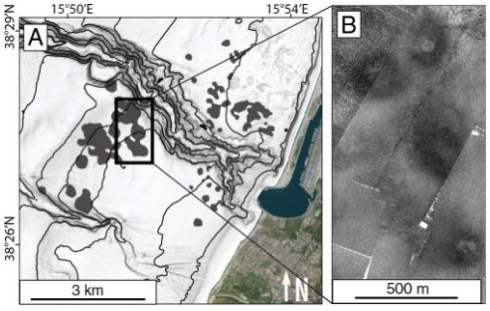

Fig. 13. Sediment disposal around the Gioia Canyon. A: Disposal areas mapped based on the distribution of the backscatter anomalies. B: Backscatter intensity associated to the dredged material, showing a distinctive "ring-like" structure.

The low sedimentation rate here allows coarse-grained, low-stand sediment to outcrop on the outer shelf and at the shelf break. The presence of comet mark fields along this portion of the continental shelf also points to the strong influence of bottom currents flowing parallel to the margin (Lupia Palmieri et al., 1997). Bottom currents may also affect the continental slope in this sector of the margin, as suggested by the presence of mound-shaped contourite deposits.

5.2. Driving factors affecting megabenthic community distribution

Multivariate analyses suggest that substrate type can be considered the main factor controlling the distribution of the different megafaunal assemblages identified, although depth and slope also contribute to the explanation of the observed patterns (Table 4). Sedimentary features, processes and community distributions will be hereafter described separately for the two main domains: 1) the canyon system; and 2) the Palmi Ridge.

5.2.1. Canyon system

Megafaunal communities dwelling in canyon heads are intuitively subject to a moderate-high degree of seafloor disturbance, given that there are higher sedimentation rates and more frequent reworking processes in these areas (Harris, 2014). The results obtained in this study reveal a total absence of megafauna on the ROV dive performed in the Petrace Canyon head, possibly indicating strong physical disturbance on the seafloor due to vigorous canyon activity, which is likely enhanced by its proximity to the fiumara mouth (about 300 m). Litter and terrestrial vegetal material commonly observed during this dive, testify to input from the nearby fiumara. Further investigations may be needed to clarify if such disturbance processes occur in all sectors of the canyon head, as only a small amount of video footage (130 m) was recorded in the Petrace Canyon.

Differently, the upper reach of the Gioia Canyon hosts a benthic assemblage largely dominated by sea pens (Assemblage 1). This finding reflects a consistent input of fine sediment supplied by fiumare along with possible organic matter enrichment and moderate current speeds. Sea pens are passive suspension feeders that rely on currents that transport organic-rich sediments. The spatial distribution of F. quadrangularis and P. rubra may reflect different disturbance processes affecting the seafloor. In this sense, at the Gioia Canyon head locally higher

sedimentation rates and turbidite flows activity forming cyclic steps may inhibit the colonization of the F. quadrangularis, whose presence was only detected in less disturbed areas, such as the Gioia Canyon margins and the shelf break. This species is considered to be a slow-growing and long-lived sea pen (Hughes, 1998), particularly vulnerable to physical stressing factors. Vetter and Dayton (1999) and Paull et al. (2010a) reported comparable observations for benthic communities in the upper reach of active shelf-indenting canyons (La Jolla and Monterey canyons respectively). In particular Paull et al. (2010a) found that frequent and severe physical seafloor disturbance, related to mass wasting events (including turbidite flows), inhibited slow-growing communities from becoming established within the axial channel of the upper Monterey Canyon.

Within the sea pen assemblage, the occurrence of L. phalangium at the shelf break may indicate the presence of strong bottom currents (Colloca et al., 2004). The distribution of this crinoid, a characteristic species of the Mediterranean muddy detritic assemblage (Bellan-Santini et al., 2002) could be also related to the presence of gravelly muddy sediments, associated with the disposal of coarse-grained material from dredging operations (see Section 5.3).

The rocky outcrops mixed with muddy bottoms found along the flanks of the Gioia Canyon, where seafloor gradients exceed 15°, provided a suitable habitat for cerianthids and shrimps (Assemblage 2). Similar assemblages have been reported on the flanks of several canyons of the northwestern Atlantic margin (Davies et al., 2014), either on bedrock covered by a veneer of fine sediment or over muddy sandy bottoms. Sea pens, commonly found on fine-grained gentle slopes and flat areas, struggle to develop over the near-vertical walls or steep surfaces (N15°) observed along the flanks of the Gioia Canyon.

On the canyon margins, below the shelf break, lower rates of hemipelagic sedimentation facilitate the colonization of the seabed by the bamboo coral I. elongata and the sea pens K. stelliferum and F. quadrangularis (Assemblage 3). Suitable habitat conditions for I. elongata include a local enrichment of food availability and low and stable sedimentation rates (Carpine and Grasshoff, 1975; Cartes et al., 2013). The assemblage found in this area includes taxa that are generally linked with compact bathyal muds (Bellan-Santini et al., 2002; Mastrototaro et al., 2013), which have also been reported along the margins of several submarine canyons (Rowe, 1971; Davies et al., 2014; Fabri et al., 2014).

5.2.2. The Palmi Ridge

The soft bottoms of the outer shelf close to the Palmi Ridge host the same sea pen assemblage found along the shallower sectors of the Gioia Canyon (Assemblage 1), reflecting the general fine grained depositional regime and the moderate hydrodynamics of the margin. Large fields of P. rubra were already recorded offshore Palmi in previous studies, mainly clustered in areas where hydrodynamic conditions provide the necessary food supply (Porporato et al., 2008).

On the other hand, the rocky outcrops of the Palmi Ridge located on the shelf break (80–100 m depth) are colonized by large specimens of the black coral A. subpinnata (Assemblage 4), suggesting the presence of more intense currents that enhance food particle supply and therefore favor the development of benthic suspension feeders. Black coral distribution, in fact, generally relates to strong hydrodynamics (Bo et al., 2008). The occurrence of large coral meadows of A. subpinnata along the southern Calabrian margin, which is less than 20 km away from our study area, was related to the hydrodynamic conditions in the Messina Strait (Bo et al., 2009).

The presence of intense currents in the area also favors the colonization of different substrates by deep-water sponges (Assemblage 5), which dwell mainly on the rocky outcrops of the upper slope. This assemblage was dominated by P. monilifera, which had a patchy distribution in elevated rocky areas. The assemblage was characterized by high abundance of sponges interspersed with flat areas, sometimes draped by a veneer of fine sediments, where the sea urchin C. cidaris was also found. The dense sponge patches observed over the rocky outcrops along the continental slope suggest a substantial availability of food particles in the southern sector. As a whole, the identified benthic assemblages indicate that moderate to intense bottom currents are affecting the seafloor of the Palmi Ridge. This is consistent with the action of the Levantine Intermediate Waters (LIW) flowing from the Messina Strait northward close to the continental margin. This water mass has previously been described flowing in the Gulf of Gioia (Marullo and Santoleri, 1986), providing food for benthic suspension feeder (Innamorati et al., 1996). The current measurements confirmed the presence of LIW in the study area flowing northward and lapping the Palmi Ridge with peak velocities of 40 cm/s (Dr. F. Falcini, personal communication).

5.3. Anthropogenic impacts and ecological relevance of the megabenthic communities

The results from this study show that the study area is affected by multiple anthropogenic activities that may influence the integrity of the described benthic assemblages. The Gioia Canyon head is located just few hundred meters off the entrance of the Gioia Tauro Harbor, one of the largest transshipment harbors in the Mediterranean Sea (Fera and De Paoli, 2012). Backscatter intensity and grain size data provide evidence of seabed alteration produced by the disposal of coarse-grained material from dredging operations in the Gioia Tauro Harbor, along the continental shelf and the canyon margins. Observations made on a survey in the late 1970s corroborate our observations; gravelly sediments collected along the continental shelf close to the harbor are attributable to dredging operations (P. Tortora, personal communication). In spite of the alteration of the seabed composition, no changes in the megafaunal community attributable to those alterations were observed in the ROV videos performed over the disposal areas. This may be due to the possibly age of the disposal, which has presumably been great enough to allow for community recovery. Furthermore, some of the high-backscatter patches found extend all the way to the canyon margins, suggesting that the disposed material could have been funneled into the canyons, thus influencing those environments, too.

The physical damage caused by trawling activities is another important human-induced alteration of the seabed in the study area. Even though no data are available about the intensity and periodicity of the commercial fishing activities in the Gulf of Gioia, the ROV observations provide clear evidence of the physical damage caused by the trawling gears on the seabed. Such damage appeared in most of the ROV video transects, including those collected along the canyon margins. Trawling activities over the soft bottom habitats surrounding the Gioia and Petrace canyons may have had an adverse impact on the distribution and abundance of the main benthic communities. Such adverse impacts may explain the low abundance of soft-bottom taxa recorded. As an example, the ROV dive that was carried out in the continental slope adjacent to the Gioia Canyon, where numerous trawl marks were counted, revealed a very scarce megafaunal composition, with only 13 individuals observed along a linear transect of almost 550 m in length.

The effects of bottom trawling on benthic marine ecosystems have been widely documented in the literature. Those effects include modifications of the habitat structure and alterations of the associated benthic community, mostly in terms of abundance, functional composition and diversity (De Groot, 1984; Mangano et al., 2013). Benthic communities dwelling in areas exposed to regular disturbances from trawling activities tend to exhibit a lower taxonomic complexity, biomass and secondary production when compared to other assemblages from areas not altered by trawlers (De Juan et al., 2007).

Regarding the conservation status of the benthic ecosystems in the study area, soft mud facies with F. quadrangularis and compact mud facies with I. elongata are listed by The General Fisheries Commission for the Mediterranean (GFCM) among the most sensitive habitats and indicative of vulnerable marine ecosystems

(VMEs) (FAO, 2009). These species are considered of relevance in terms of management priorities (GFCM, 2009), since they provide essential habitats for certain crustacean species of commercial interest. Their role in increasing local biomass and diversity by providing increases in habitat heterogeneity is well known (Maynou and Cartes, 2011). Furthermore, these two species are extremely vulnerable to the effects of commercial fisheries (Cartes et al., 2004) and it is believed that F. quadrangularis and I. elongata have already disappeared from many trawled bottoms of the Western Mediterranean Sea (Sardà et al., 2004).

The rocky outcrops located at the Palmi Ridge host other taxa of high conservation value, such as black corals and deep sea sponges. These are examples of engineering taxa known to play an important functional role in the sustainability of deep-sea benthic ecosystems, supporting high rates of local biodiversity (Bo et al., 2012a and 2012b). Deep-sea sponge aggregations are also included in the OSPAR Commission list of threatened and/or declining habitats that require protection (http://www.ospar.org). These communities are not directly threatened by trawling activities, although the large number of discarded fishing lines observed in the video images indicates the existence of a certain fishing pressure in this area.

6. Conclusions

The multidisciplinary study of the upper reach of the Gioia Canyon and surrounding area, based on multibeam data, high resolution seismic profiles, sediment samples and ROV video data, documented benthic communities, morpho-sedimentary features and processes affecting the seafloor. The results from this study show a key role of morpho-sedimentary processes on the benthic community composition and distribution, and highlight the value of multi-disciplinary approaches in the study of complex environments such as submarine canyons.

In the study area, a combination of geological–structural factors (the tectonic setting of the margin and the distribution of the major morphological features) and the present-day sedimentary regime control the distribution of benthic fauna. We distinguished three areas where diverse environmental conditions determine the presence of distinct megabenthic assemblages: 1) the upper reaches of the Gioia and Petrace canyons, from the canyon heads to the shelf break; 2) the slope sectors of the Gioia Canyon; and 3) the Palmi Ridge.

1) High sedimentation rates on the continental shelf result in the prevalence of soft sedimentary bottoms, which are colonized by an assemblage dominated by sea pens, both inside and outside the canyon. Physical disturbance on the seafloor, related to high sedimentation rates and the occasional occurrence of turbidity flows, may limit megafauna colonization along specific sectors of the canyon system, thus explaining the lack of megafauna at the head of Petrace Canyon.
2) Beyond the shelf break, lower sedimentation rates and more stable environmental conditions support benthic communities that include I. elongata, K. stelliferum and F. quadrangularis, species favoring habitat heterogeneity and recognized as indicative of vulnerable marine ecosystems (VMEs).
3) On the Palmi Ridge the presence of more varied substrates and high energy nutrient-rich currents associated to the LIW coming from the Messina Strait create suitable conditions for hard-bottom assemblages, including the black coral A. subpinnata and deep-sea sponge fields.

The diffuse trawl marks observed on the seafloor of the continental shelf and slope, including the canyon margins, indicate fishing pressure in the study area, which could explain local low abundances of soft-bottom megabenthic taxa. Since the soft-bottoms of the canyon margins and flanks host the sea pen F. quadrangularis and the octocoral I. elongata, these areas should deserve special attention for preservation of such species that are considered of high conservation value.

Acknowledgments

This research was performed in the framework of the Flagship Project RITMARE (SP4-WP2-A1). The authors wish to acknowledge the captains and crews of R/V Urania for their critical assistance in the collection of data and Dr. Andrea Gori from the University of Barcelona for his help in the video data analyses. We are also grateful to Dr. Iosune Uriz, Dr. Rafael Sardá (CSIC) and Dr. Pablo J. López-González of University of Sevilla for their help for taxonomical identification. We would like to thank two anonymous reviewers, whose suggestions greatly improved the manuscript. We are grateful to Dr. Vince Guida (NOAA-NEFSC) for the English revision.

References

Allen, S.E., Durrieu de Madron, X., 2009. A review of the role of submarine canyons in deep-ocean exchange with the shelf. Ocean Sci. Discuss. 6 (2), 1369–1406.

Allen, S.E., Vindeirinho, C., Thomson, R.E., Foreman, M.G., Mackas, D.L., 2001. Physical and biological processes over a submarine canyon during an upwelling event. Can. J. Fish. Aquat. Sci. 58 (4), 671–684.

Barone, A., Fabbri, A., Rossi, S., Sartori, R., 1982. Geological structure and evolution of the marine areas adjacent to the Calabrian arc. Earth Evol. Sci. 3, 207–221.

Bellan-Santini, D., Bellan, G., Bittar, G., Harmelin, J.G., Pergent, G., 2002. Handbook for Interpreting Types of Marine Habitat for the Selection of Sites to Be Included in the National Inventories of Natural Sites of Conservation Interest, UNEP Report, Tunis. p. 217.

Bo, M., Bertolino, M., Bavestrello, G., Canese, S., Giusti, M., Angiolillo, M., ... Taviani, M., 2012b. Role of deep sponge grounds in the Mediterranean Sea: a case study in southern Italy. Hydrobiologia 687 (1), 163–177.

Bo, M., Canese, S., Spaggiari, C., Pusceddu, A., Bertolino, M., Angiolillo, M., ... Bavestrello, G., 2012a. Deep coral oases in the South Tyrrhenian Sea. PLoS One 7 (11), e49870.

Bo, M., Bavestrello, G., Canese, S., Giusti, M., Salvati, E., Angiolillo, M., Greco, S., 2009. Characteristics of a black coral meadow in the twilight zone of the Central Mediterranean Sea. Mar. Ecol. Prog. Ser. 397, 53–61.

Bo, M., Tazioli, S., Spanò, N., Bavestrello, G., 2008. Antipathella subpinnata (Antipatharia, Myriopathidae) in Italian seas. Ital. J. Zool. 75 (2), 185–195.

Brandt, P., Rubino, A., Alpers, W., Backhaus, J.O., 1997. Internal waves in the Strait of Messina studied by a numerical model and synthetic aperture radar images from the ERS 1/2 satellites. J. Phys. Oceanogr. 27 (5), 648–663.

Canals, M., Puig, P., de Madron, X.D., Heussner, S., Palanques, A., Fabres, J., 2006. Flushing submarine canyons. Nature 444 (7117), 354–357.

Carpine, C., Grasshoff, M., 1975. Les gorgonaires de la Méditerranée. Bull. Inst. Océanogr. Monaco 71 (1430) (fondation Albert I^{er}, prince de Monaco). (140 pp).

Cartes, J.E., Lolacono, C., Mamouridis, V., López-Pérez, C., Rodríguez, P., 2013. Geomorphological, trophic and human influences on the bamboo coral Isidella elongata assemblages in the deep Mediterranean: to what extent does Isidella form habitat for fish and invertebrates? Deep-Sea Res. I Oceanogr. Res. Pap. 76, 52–65.

Cartes, J.E., Maynou, F., Sardà, F., Company, J.B., Lloris, D., Tudela, S., 2004. The Mediterranean deep-sea ecosystems: an overview of their diversity, structure, functioning and anthropogenic impacts. The Mediterranean Deep-Sea Ecosystems: An Overview Of Their Diversity, Structure, Functioning And Anthropogenic Impacts, With A Proposal For Conservation. IUCN, Málaga and WWF, Rome, pp. 9–38.

Cartigny, M.J., Postma, G., van den Berg, J.H., Mastbergen, D.R., 2011. A comparative study of sediment waves and cyclic steps based on geometries, internal structures and numerical modeling. Mar. Geol. 280 (1), 40–56.

Casalbore, D., Bosman, A., Ridente, D., Chiocci, F.L., 2014. Coastal and submarine landslides in the tectonically-active Tyrrhenian Calabrian Margin (Southern Italy): examples and geohazard implications. Submarine Mass Movements and Their Consequences. Springer International Publishing, pp. 261–269.

Casalbore, D., Chiocci, F.L., Mugnozza, G.S., Tommasi, P., Sposato, A., 2011. Flash-flood hyperpycnal flows generating shallow-water landslides at Fiumara mouths in Western Messina Strait (Italy). Mar. Geophys. Res. 32 (1–2), 257–271.

Chiocci, F.L., Ridente, D., 2011. Regional-scale seafloor mapping and geohazard assessment. the experience from the Italian project MaGIC (marine geohazards along the Italian coasts). Mar. Geophys. Res. 32 (1–2), 13–23.

Chiocci, F.L., D'Angelo, S., Orlando, L., Pantaleone, A., 1989. Evolution of the Holocene shelf sedimentation defined by high-resolution seismic stratigraphy and sequence analysis (Calabro–Tyrrhenian continental shelf). Mem. Soc. Geol. Ital. 48, 359–380.

Clarke, K., Gorley, R., 2006. PRIMER v6: User Manual/Tutorial. Primer-E Ltd, Plymouth.

Colantoni, P., Gennesseaux, M., Vanney, J.R., Ulzega, A., Melegari, G., Trombetta, A., 1992. Processi dinamici del canyon sottomarino di gioia tauro (Mare Tirreno). Giorn. Geol. 3 (54/2), 199–213.

Colloca, F., Carpentieri, P., Balestri, E., Ardizzone, G.D., 2004. A critical habitat for Mediterranean fish resources: shelf-break areas with Leptometra phalangium (Echinodermata: Crinoidea). Mar. Biol. 145 (6), 1129–1142.

Critelli, S., Le Pera, E., 1998. Post-Oligocene sediment-dispersal systems and unroofing history of the Calabrian microplate, Italy. Int. Geol. Rev. 40 (7), 609–637. http://dx.doi.org/10.1080/00206819809465227.

D'Alessandro, L., Davoli, L., Lupia Palmieri, E., Raffi, R., 2002. Natural and anthropogenic factors affecting the recent evolution of beaches in Calabria (Italy). In: R.J., A. (Ed.), Applied Geomorphology: Theory and Practice. 10, pp. 397–429.

Davies, J.S., Howell, K.L., Stewart, H.A., Guinan, J., Golding, N., 2014. Defining biological assemblages (biotopes) of conservation interest in the submarine canyons of the South West approaches (offshore United Kingdom) for use in marine habitat mapping. Deep-Sea Res. II Top. Stud. Oceanogr. 104, 208–229.

De Groot, S.J., 1984. The impact of bottom trawling on benthic fauna of the North Sea. Ocean Manage. 9 (3), 177–190.

De Juan, S., Thrush, S.F., Demestre, M., 2007. Functional changes as indicators of trawling disturbance on a benthic community located in a fishing ground (NW Mediterranean Sea). Mar. Ecol. Prog. Ser. 334, 117–129.

De Leo, F.C., Smith, C.R., Rowden, A.A., Bowden, D.A., Clark, M.R., 2010. Submarine canyons: hotspots of benthic biomass and productivity in the deep sea. Proc. R. Soc. B Biol. Sci. 277, 2783–2792.

De Leo, F.C., Vetter, E.W., Smith, C.R., Rowden, A.A., McGranaghan, M., 2014. Spatial scale-dependent habitat heterogeneity influences submarine canyon macrofaunal abundance and diversity off the main and northwest Hawaiian Islands. Deep-Sea Res. II Top. Stud. Oceanogr. 104, 267–290.

Doglioni, C., Innocenti, F., Morellato, C., Procaccianti, D., Scrocca, D., 2004. On the Tyrrhenian Sea opening. Mem. Descr. Carta. Geol. Ital. 64, 147–164.

Duffy, G.A., Lundsten, L., Kuhnz, L.A., Paull, C.K., 2014. A comparison of megafaunal communities in five submarine canyons off Southern California, USA. Deep-Sea Res. II Top. Stud. Oceanogr. 104, 259–266.

Fabbri, A., Ghisetti, F., Vezzani, L., 1980. The Peloritani–Calabria range and the Gioia basin in the Calabrian arc (Southern Italy): relationships between land and marine data. Geol. Romana 19, 131–150.

Fabri, M.C., Pedel, L., Beuck, L., Galgani, F., Hebbeln, D., Freiwald, A., 2014. Megafauna of vulnerable marine ecosystems in French mediterranean submarine canyons: spatial distribution and anthropogenic impacts. Deep-Sea Res. II Top. Stud. Oceanogr. 104, 184–207.

FAO, 2009. Report of the Technical Consultation on International Guidelines for the Management of Deep-Sea Fisheries in the High Seas. 881. FAO, p. 98.

Fera, G., De Paoli, R.G., 2012. Gioia Tauro–Rosarno: The Harbour Without a City-Port. Portus Plus, p. 3.

Fonseca, L., Calder, B., 2005. Geocoder: an efficient backscatter map constructor. Proceedings of the US Hydrographic Conference San Diego, CA, March 29–31, 2005.

Galparsoro, I., Borja, Á., Legorburu, I., Hernández, C., Chust, G., Liria, P., Uriarte, A., 2010. Morphological characteristics of the Basque continental shelf (Bay of Biscay, Northern Spain); their implications for Integrated Coastal Zone Management. Geomorphology 118, 314–329.

Gamberi, F., Marani, M., 2006. Hinterland geology and continental margin growth: the case of the Gioia Basin (Southeastern Tyrrhenian Sea). Geol. Soc. Lond., Spec. Publ. 262 (1), 349–363.

Gamberi, F., Marani, M., 2008. Controls on Holocene deep-water sedimentation in the northern Gioia Basin, Tyrrhenian Sea. Sedimentology 55 (6), 1889–1903.

GFCM, 2009. Criteria for the Identification of Sensitive Habitats of Relevance for the Management of Priority Species (General Fisheries Commission for the Mediterranean) Malaga.

Gori, A., Orejas, C., Madurell, T., Bramanti, L., Martins, M., Quintanilla, E., ... Gili, J.M., 2013. Bathymetrical distribution and size structure of cold-water coral populations in the Cap de Creus and Lacaze–Duthiers canyons (Northwestern Mediterranean). Biogeosciences 10 (3), 2049–2060.

Harris, P.T., 2014. Shelf and deep-sea sedimentary environments and physical benthic disturbance regimes: A review and synthesis. Mar. Geol. 353, 169–184.

Harris, P.T., Whiteway, T., 2011. Global distribution of large submarine canyons: geomorphic differences between active and passive continental margins. Mar. Geol. 285 (1), 69–86.

Hughes, D.J., 1998. Sea Pens and Burrowing Megafauna (Vol. III): An Overview of Dynamics and Sensitivity Characteristics for Conservation Management of Marine SACs. Scottish Association of Marine Science (UK Marine SAC's Project) (105 pp). Huvenne, V.A., Tyler, P.A., Masson, D.G., Fisher, E.H., Hauton, C., Hühnerbach, V., ... Wolff, G.A., 2011. A picture on the wall: innovative mapping reveals cold-water coral refuge in submarine canyon. PLoS One 6 (12), e28755.

Innamorati, M., Massi, L., Nuccio, C., 1996. Indipendenza delle cenosi fitoplanctoniche dalle masse d'acqua circostanti le isole eolie. Atti del XI Congresso della Associazione Italiana di Oceanologia e Limnologia, pp. 645–654.

Kao, S.J., Milliman, J.D., 2008. Water and sediment discharge from small mountainous rivers, Taiwan: The roles of lithology, episodic events, and human activities. J. Geol. 116 (5), 431–448.

Lamb, M.P., Parsons, J.D., Mullenbach, B.L., Finlayson, D.P., Orange, D.L., Nittrouer, C.A., 2008. Evidence for superelevation, channel incision, and formation of cyclic steps by turbidity currents in Eel Canyon, California. Geol. Soc. Am. Bull. 120 (3–4), 463–475.

Lupia Palmieri, E., D'Alessandro, L., Fredi, P., Raffi, R., 1997. Atlante delle spiagge italiane: Dinamismo-Tendenza evolutiva-Opere umane (FOGLIO 245 PALMI. S.EL.CA., Firenze).

Mangano, M.C., Kaiser, M.J., Porporato, E.M., Spanò, N., 2013. Evidence of trawl disturbance on mega-epibenthic communities in the Southern Tyrrhenian Sea. Mar. Ecol. Prog. Ser. 475, 101–117.

Martorelli, E., Falese, F., Chiocci, F.L., 2014. Overview of the variability of Late Quaternary continental shelf deposits of the Italian peninsula. Geol. Soc. Lond. Mem. 41 (1), 171–186.

Marullo, S., Santoleri, R., 1986. Fronts and internal currents at the northern mouth of the Strait of Messina. Il Nuovo Cimento C 9 (3), 701–713.

Masson, D.G., Huvenne, V.A.I., de Stigter, H.C., Arzola, R.G., LeBas, T.P., 2011. Sedimentary processes in the middle Nazaré Canyon. Deep-Sea Res. II Top. Stud. Oceanogr. 58 (23), 2369–2387.

Mastrototaro, F., Maiorano, P., Vertino, A., Battista, D., Indennidate, A., Savini, A., ... D'Onghia, G., 2013. A facies of Kophobelemnon (Cnidaria, Octocorallia) from Santa Maria di Leuca coral province (Mediterranean Sea). Mar. Ecol. 34 (3), 313–320. Maynou, F., Cartes, J.E., 2011. Effects of Trawling on Fish and Invertebrates from Deep-Sea Coral Facies of Isidella elongata in the Western Mediterranean.

McClain, C.R., Barry, J.P., 2010. Habitat heterogeneity, disturbance, and productivity work in concert to regulate biodiversity in deep submarine canyons. Ecology 91 (4), 964–976.

Morelli, E., Martorelli, E., Chiocci, F.L., 2013, April. Morphostructure and controlling factors on the past and present Gioia–Mesima submarine/channel system (Southern Tyrrhenian Sea, Italy). EGU General Assembly Conference Abstracts. Vol. 15, p. 1030.

Okey, T.A., 1997. Sediment flushing observations, earthquake slumping, and benthic community changes in Monterey Canyon head. Cont. Shelf Res. 17 (8), 877–897.

Okey, T.A., 2003. Macrobenthic colonist guilds and renegades in Monterey Canyon (USA) drift algae: partitioning multidimensions. Ecol. Monogr. 73 (3), 415–440.

Paull, C.K., Schlining, B., Ussler III, W., Lundste, E., Barry, J.P., Caress, D.W., ... McGann, M., 2010a. Submarine mass transport within Monterey Canyon: benthic disturbance controls on the distribution of chemosynthetic biological communities. Submarine Mass Movements and Their Consequences. Springer, Netherlands, pp. 229–246.

Paull, C.K., Ussler III, W., Caress, D.W., Lundsten, E., Covault, J.A., Maier, K.L., ... Augenstein, S., 2010b. Origins of large crescent-shaped bedforms within the axial channel of Monterey Canyon, offshore California. Geosphere 6 (6), 755–774.

Poff, N.L., Allan, J.D., Bain, M.B., Karr, J.R., Prestegaard, K.L., Richter, B.D., ... Stromberg, J.C., 1997. The natural flow regime. Bioscience 769–784.

Poppe, L. J., Lewis, R. S., Knebel, H. J., Haase, E. A., Parolski, K. F., DiGiacomo-Cohen, M. L. (2001). Sidescan sonar images, surficial geologic interpretations, and bathymetry of New Haven Harbor, Connecticut, and the New Haven dumping ground, north-Central Long Island Sound. US Geological Survey Geologic Investigations Series Map I-2736, 2.

Porporato, E., Mangano, M.C., De Domenico, F., Giacobbe, S., Spanò, N., 2008. Addensamenti di pennatulacei nello stretto di Messina. Biol. Marina Mediterranea 15 (1), 284–285.

Puig, P., Palanques, A., 1998. Temporal variability and composition of settling particle fluxes on the Barcelona continental margin (Northwestern Mediterranean). J. Mar. Res. 56 (3), 639–654.

Puig, P., Palanques, A., Martín, J., 2014. Contemporary sediment-transport processes in submarine canyons. Ann. Rev. Mar. Sci. 6, 53–77.

Ramirez-Llodra, E., Brandt, A., Danovaro, R., De Mol, B., Escobar, E., German, C.R., ... Vecchione, M., 2010. Deep, diverse and definitely different: unique attributes of the world's largest ecosystem. Biogeosciences 7, 2851–2899.

Rowe, G.T., 1971. Observations on bottom currents and epibenthic populations in Hatteras Submarine Canyon. Deep Sea Research and Oceanographic Abstracts 18(6). Elsevier, pp. 569–581.

Rowe, G.T., Polloni, P.T., Haedrich, R.L., 1982. The deep-sea macrobenthos on the continental margin of the Northwest Atlantic Ocean. Deep Sea Res. Part A 29 (2), 257–278.

Sabato, L., Tropeano, M., 2004. Fiumara: a kind of high hazard river. Phys. Chem. Earth A/B/C 29 (10), 707–715.

Sardà, F., Calafat, A., Flexas, M., Tselepides, A., Canals, M., Espino, M., Tursi, A., 2004. An introduction to Mediterranean deep-sea biology. Sci. Mar. 68 (S3), 7–38.

Shepard, F.P., Dill, R.F., 1966. Submarine Canyons and Other Sea Valleys. Rand McNally, USA.

Sorriso-Valvo, G., Terranova, O., 2006. The Calabrian fiumara streams. Z. Geomorphol. Land Degrad. Suppl. 143, 109–125.

Sparnocchia, S., Gasparini, G.P., Astraldi, M., Borghini, M., Pistek, P., 1999. Dynamics and mixing of the Eastern Mediterranean outflow in the Tyrrhenian basin. J. Mar. Syst. 20 (1), 301–317.

Tortorici, L., Monaco, C., Tansi, C., Cocina, O., 1995. Recent and active tectonics in the Calabrian arc (Southern Italy). Tectonophysics 243 (1), 37–55.

Van Oevelen, D., Soetaert, K., García, R., De Stigter, H.C., Cunha, M.R., Pusceddu, A., Danovaro, R., 2011. Canyon conditions impact carbon flows in food webs of three sections of the Nazaré canyon. Deep-Sea Res. II Top. Stud. Oceanogr. 58 (23), 2461–2476.

Van Rein, H., Brown, C.J., Quinn, R., Breen, J., Schoeman, D., 2011. An evaluation of acoustic seabed classification techniques for marine biotope monitoring over broad-scales (N1 km^2) and meso-scales (10 m^2–1 km^2). Estuar. Coast. Shelf Sci. 93 (4), 336–349.

Vetter, E.W., Dayton, P.K., 1998. Macrofaunal communities within and adjacent to a detritus-rich submarine canyon system. Deep-Sea Res. II 45 (1–3), 25–54.

Vetter, E.W., Dayton, P.K., 1999. Organic enrichment by macrophyte detritus, and abundance patterns of megafaunal populations in submarine canyons. Mar. Ecol. Prog. Ser. 186, 137–148.

Vetter, E.W., Smith, C.R., De Leo, F.C., 2010. Hawaiian hotspots: enhanced megafaunal abundance and diversity in submarine canyons on the oceanic islands of Hawaii. Mar. Ecol. 31 (1), 183–199.

Xu, J.P., Swarzenski, P.W., Noble, M., Li, A.C., 2010. Event-driven sediment flux in Hueneme and Mugu submarine canyons, Southern California. Mar. Geol. 269, 74–88.

Zaniboni, F., Armigliato, A., Pagnoni, G., Tinti, S., 2014. Continental margins as a source of tsunami hazard: the 1977 Gioia Tauro (Italy) landslide–tsunami investigated through numerical modeling. Mar. Geol. 357, 210–217.